

## LOCAL RESISTANCE OF SURFACE MOUNTED OBSTACLES

Z. Chára\*, B. Hoření\*

**Summary:** *The influence of surface mounted obstacles on free level of channel flow is discussed. The obstacles of square cross section are placed sequentially along a hydraulic flume and perpendicularly to the flow direction across the whole channel width. Three various spacing between the obstacles -  $5H$ ,  $11H$  and  $23H$  ( $H$  is height of the obstacle) were tested for different flow discharges. The surface levels were recorded and the results were compared with numerical simulations. Based on the experimental data and numerical simulations the resistance coefficients of the individual obstacles were determined.*

### 1. Introduction

Flow over macro wall roughness elements, which have constant longitudinal spacing and height along the channel can be referred as the wake-interfering or hyper-turbulent flow (Morris, 1959). Due to the vortices generated on the rough elements such flow is much more turbulent and energy consuming compared with flow over smooth surface. This phenomenon can be useful to dissipate the kinetic energy mainly in mountain areas where the slopes of natural streams are relatively high. On the other hand the transverse bars can be used for a revitalization of straight section of artificially adapted channels. To determine the effect of the macro rough elements on the hydraulic parameters it is necessary to know the resistance coefficients of the elements in dependence on the position and flow parameters. There exist a lot of papers dealing with the problem of turbulent flow over rib-roughened plates or in channels (Casarsa & Arts, 2002; Cui et al., 2003; Kameda et al., 2004; Leonardi et al., 2003; Okamoto et al., 1993). But most of them are devoted to the flow in closed conduits.

The presented paper is focused on the determination of the local resistance of transverse rectangular bars of square cross section and their influence on the turbulent flow in a hydraulic flume.

### 2. Experimental part

The experiments were performed in the hydraulic flume of a cross section  $0.4 \times 0.4$  m and a length 24 m. Side walls are made from glass tables, the bottom is covered by a smooth

---

\* Ing. Zdeněk Chára, CSc., Ing. Bohumír Hoření, CSc.: Institute of Hydrodynamics AS CR; Pod Patankou 30/5, 166 12 Praha 6; tel.: + 420.233323748, fax: + 420.233324361; e-mail: chara@ih.cas.cz

plastic layer. The slope of the flume was set to zero. The rectangular bars of the cross section  $H \times H$  ( $H=5\text{ cm}$ ) were placed on the channel bottom. Three mutual distances of the bars were investigated –  $5H$ ,  $11H$  and  $23H$ , see Fig. 1. The details of the experimental runs are summarized in Table 1.

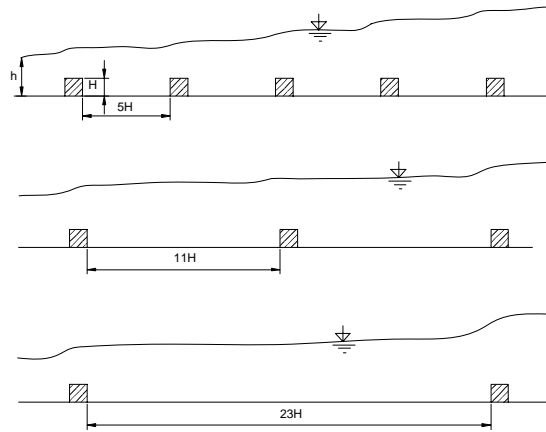


Fig. 1 Schematic view of the tested roughness

Tab.1 Hydraulic parameters

Spacing	Number of elements / total length of rough part	Experiment					Numerical simulation		
		Q [l/s]					Q [l/s]		
		14	22	27	33	39	14	27	39
5H	21 / 6 m	✓	✓	✓	✓	✓	✓	✓	✓
11H	21 / 12 m	✓	✓	✓	✓	✓		✓	
23H	13 / 14.4 m	✓	✓	✓	✓	✓		✓	

The flow depths were measured in the middle of each gap with help of an ultrasound sensor Pepperl-Fuchs UC500-30GM-V1. The sensor was mounted on a holder travelling along the channel on a guide rail. Flow rates were measured by an inductive flow meter placed on a delivery pipe. Downstream the last bar the flow was supercritical (critical conditions occurred close to the last bar). The data of flow depths and flow rates were recorded via A/D PCMCIA card National Instruments.

### 3. Numerical simulations

The numerical simulations were carried out by a commercial program Fluent 6.2. An unstructured (tri-quad) mesh of the edge size 5 mm was used in the whole computational domain. The roughness parts of the domain were built up identically as on the physical model. The standard two-dimensional  $k-\epsilon$  model and the volume of fluid (VOF) model solving the free surface were adopted. The VOF model is a surface-tracking technique applied to a fixed Eulerian mesh. It is designed for two or more immiscible fluids where the position of the

interface between the fluids is of interest. In the VOF model a single set of momentum equations is shared by the fluids, and the volume fraction of each of the fluids in each computational cell is tracked throughout the domain.

The computational domain started 3 m upstream of the bar sequence and ended on the last bar. The number of cells depended on tested geometry and varied from 200 000 to 300 000 elements. To accelerate the numerical procedure and quickly balance an amount of liquid and air phases the laminar model was used on beginning of the computations. After that the solver was switched to the standard k- $\epsilon$  model performing unsteady flow calculation with time step of 0.001 sec. The simulations were performed on a computer IBM with 32 GB RAM and equipped with four processors Power 5+.

Together with the two-dimensional solution a simple one-dimensional HEC-RAS calculation was tested, too. In the HEC-RAS the channel bottom was modelled either as macro rough (including all individual bars) or as smooth rough bed. In the case of the macro rough bed the Manning's resistance coefficient was set to  $n=0.01$  (we supposed smooth surfaces on the bed and on the bars, respectively). In the second case (the smooth roughness) the Manning's coefficient was determined from the force balance (calculated from pressure and shear stress distribution on the individual bars) and from the momentum conservation.

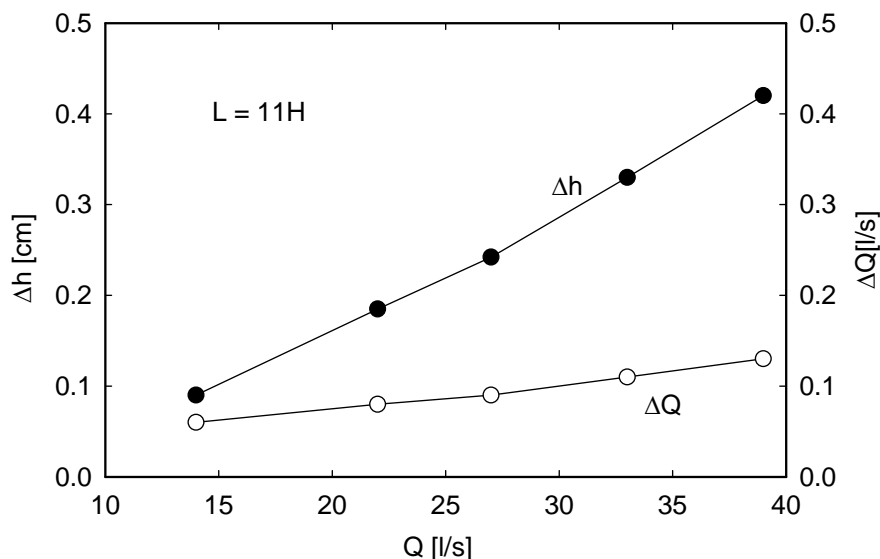


Fig. 2 Root mean square of the flow depths and flow discharges

#### 4. Results and discussion

The experimental results relied on the measurement of flow discharges and flow depths on the physical model. Unfortunately the hydraulic system was not disturbances free, both the flow discharges and depths slightly fluctuated. The dependency of the root mean square of the flow discharge and flow depth in dependency on mean value of discharge is shown in Fig. 2 for  $L=11H$ . While the fluctuations of the flow discharge are nearly constant, the fluctuations of flow depth are increasing with increasing flow discharges but the relative values of the depth fluctuations normalized by the flow depths are below 3%.

Profiles of the free surface for two discharges –  $Q=14$  and  $33$  l/s for all geometrical arrangements are shown in Fig. 3. The origin of the longitudinal axes is set to the centre of the last bar (in flow direction), the origin of the vertical axes lies on the channel bottom. The solid lines present the solution of HEC-RAS software for spacing  $L=23H$  and for macro rough bed. As can be expected this HEC-RAS approximation considerably undervalues the measured data because this approach does not take into account the influence of turbulent dissipation on single bars.

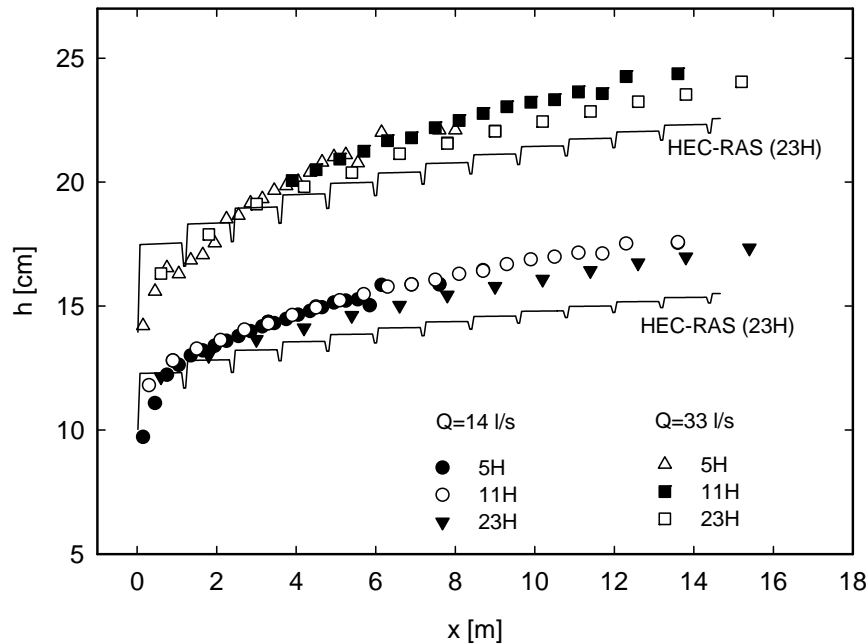
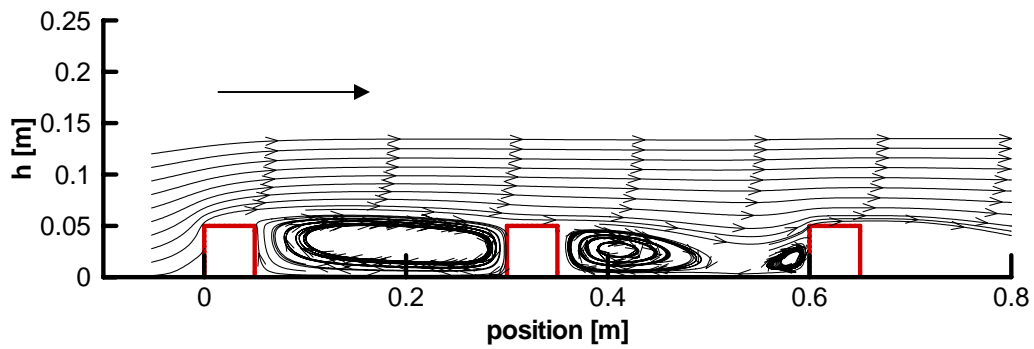
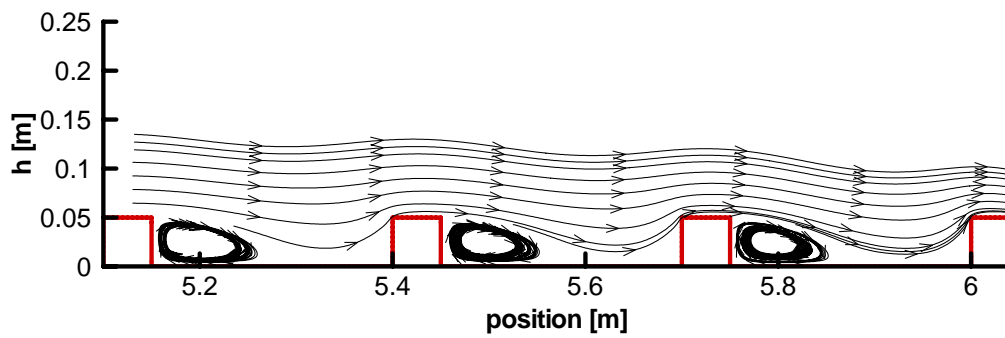
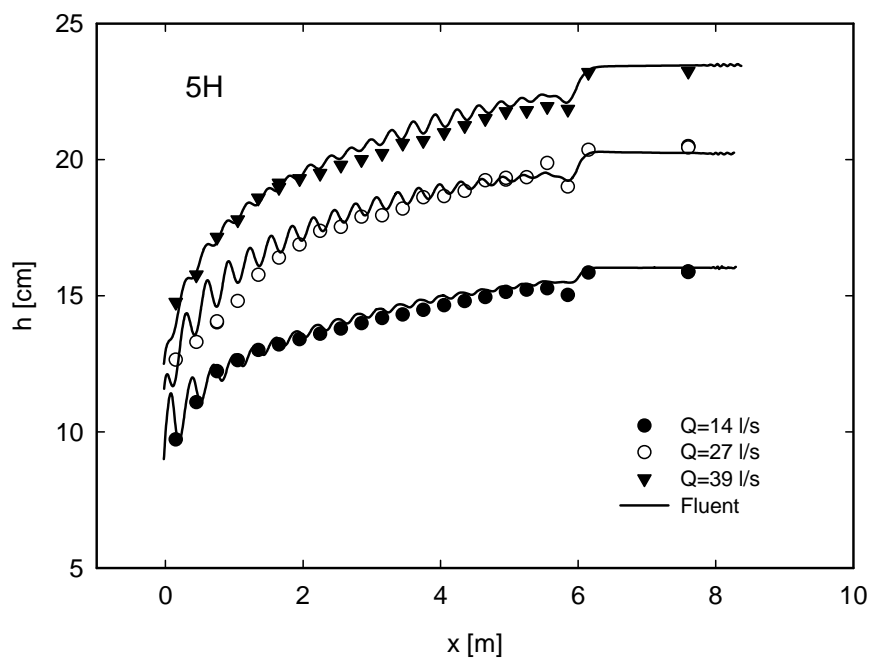


Fig. 3 Measured profiles of free surface levels

As was mentioned above the numerical simulations were performed by the program Fluent for the identical hydraulic conditions and geometric arrangements (shape, size and numbers of the bars) as on the physical model. The profiles of free levels were calculated by the VOF method, where two phases (air and water) were included. Examples of the streamlines between the bars are shown in Figs. 4a and 4b for the spacing  $L=5H$  and the discharge  $Q=27$  l/s. Fig. 4a shows the first (upstream) bars sequence, Fig. 4b shows the final part (flow direction in Figs. 4a,b is from the left to the right). A vortex is formed inside the whole cavity between the first bars (Fig. 4a). Such flow situation results in a pressure decrease on the front face of the second bar and consequently the pressure force acting on the second bar is much less or even negative compare to others. On the other hand the vortex zones behind the last but one bars (Fig. 4b) are much smaller, the streamlines are pushed down to the channel bottom and the pressure forces acting on the front faces of the bars are increasing which results in a wavy shape of the free surface near the end of the rough section. The pressure forces as well as tangential forces were calculated by an integrating of the pressure and shear stress distribution on the bar and in the cavity. The tangential forces are much smaller then the pressure forces.

Comparison between the measured and calculated (Fluent simulation) profiles of the free surface for bar distance  $L=5H$  is shown in Fig. 5, and for  $L=11H$  and  $23H$  in Fig. 6. As can be seen a very good coincidence of the measured and simulated profiles was achieved including

Fig. 4a Streamlines for  $L=5H$  and  $Q=27$  l/s – first bar sequenceFig. 4b Streamlines for  $L=5H$  and  $Q=27$  l/s – last bar sequenceFig. 5 Comparison between measured and calculated free surface profiles for  $L=5H$

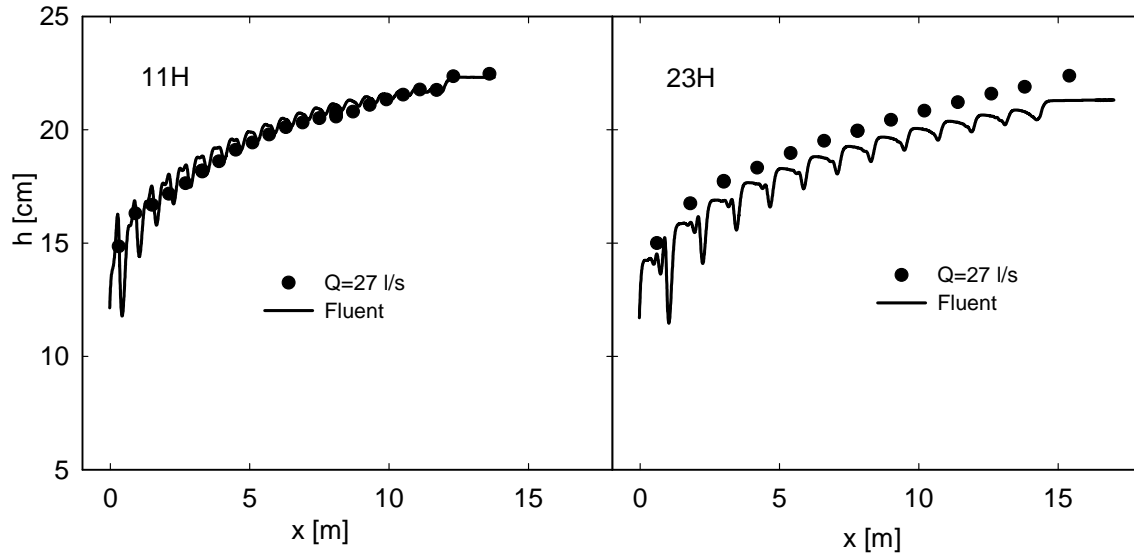


Fig. 6 Comparison between measured and calculated free surface profiles for  $L=11H$  and  $23H$

the free level upstream the rough part for  $L=5H$  and  $11H$ . Surprisingly the Fluent simulation undervalued the measured free surface levels for  $L=23H$  but the measured and simulated profiles are more or less parallel and therefore also the forces acting on the bars (determined either from momentum or force balance) are practically identical. The reason why the Fluent data lie below the measured ones could be explained by an improper output condition of the computational domain. While on the physical model the channel flow continues downstream the last bar, the computational domain simply ends on the last bar. Therefore in the numerical model the critical flow depth is shifted slightly upstream and in result the calculated free surface is lower.

An estimation of the increase of the free surface due to the transverse bars can be done using the momentum conservation. Consider the bar in a steady open channel flow. For prismatic channel of unit width the drag force on the bar can be calculated from the following equation (neglecting the bed friction)

$$C_D \frac{1}{2} \rho U^2 a = \rho \left( \frac{1}{2} g h_1^2 + \beta \frac{Q^2}{h_1} \right) - \rho \left( \frac{1}{2} g h_2^2 + \beta \frac{Q^2}{h_2} \right) \quad (1)$$

where  $a$  is height of the bars,  $C_D$  is drag coefficient,  $U$  is flow velocity at the bar,  $h_1$  and  $h_2$  are flow depths upstream and downstream the bar,  $Q$  is discharge,  $\beta$  is Boussinesq coefficient,  $\rho$  is fluid density and  $g$  is gravitational acceleration. To determine the flow depth difference between the profiles 1 and 2 it is necessary to know the value of the drag coefficient.

The total drag coefficient was determined both from the measured profiles of free surface and from the numerical simulations. If the surface elevations are known, the drag coefficient can be calculated from the Eq. 1 or the drag coefficient can be determined directly from the force balance. Fig. 7 shows the values of drag coefficient calculated from the measured profiles of the free surfaces using Eq. 1. The scatter of the data is due to the water level fluctuations, nevertheless the drag coefficient can be approximated by a horizontal line except the data on the first two bars, where the flow is completely different (see Fig. 4a). The drag

coefficients are  $C_D \sim 0.59$  for spacing  $L=5H$ ,  $C_D \sim 1.02$  for  $L=11H$  and  $C_D \sim 1.51$  for  $L=23H$ . Since the flow depths at the bars are not equal, that depth difference results in an additional pressure force acting on the individual bar. Therefore the drag coefficients (determined from the Eq. 1 or from the force balance) include also the influence of depth difference on the bar and their values can be somewhat different compare to the drag coefficients determined in closed channels or wind tunnels.

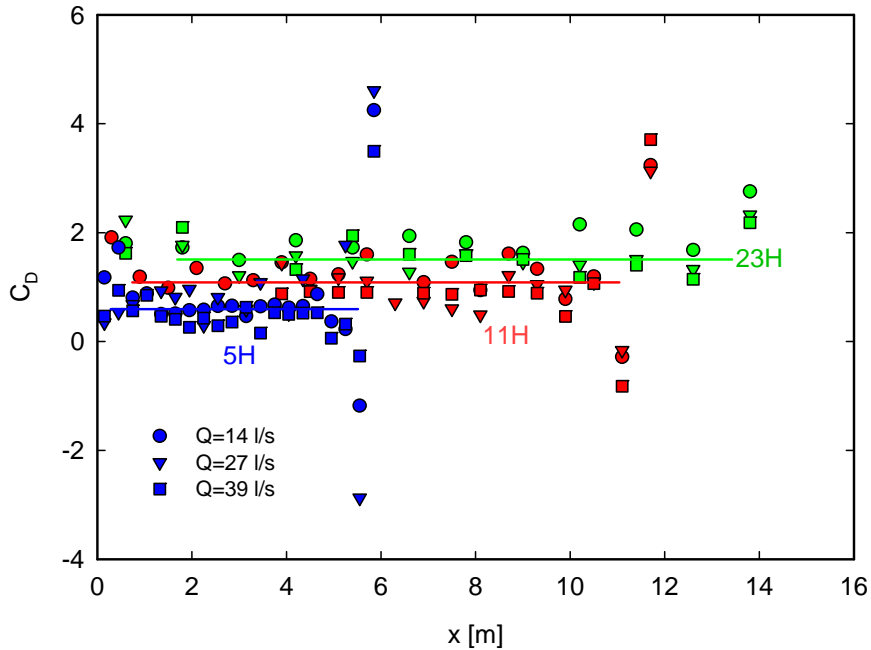


Fig. 7 Drag coefficients for different bar spacing (experimental data)

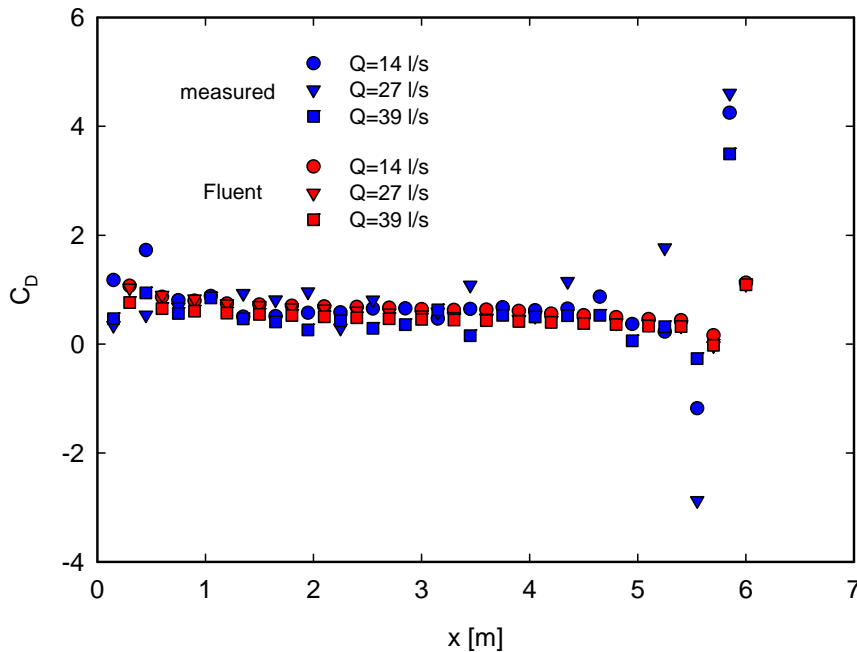


Fig. 8 Drag coefficients determined form measured depths and from

Fig. 8 shows a comparison between the drag coefficients determined from the measured data and of the coefficients determined from Fluent simulations for  $L=5H$ . The results correspond quite well, but the Fluent data seems to be slightly increasing in the flow direction.

In a hydraulic practise a usual way how to determine the flow resistance is via the Chezy's law and Manning's coefficient,  $n$ .

$$U_{mean} = \frac{1}{n} R^{\left(\frac{2}{3}\right)} i^{\left(\frac{1}{2}\right)} \quad (2)$$

where  $R$  is hydraulic radius and  $i$  is friction slope.

An assessment of the Manning's coefficient was done from the momentum conservation and provided that the flow exists only above the bars (the flow inside the cavities was not considered). For such assumptions the values of Manning's coefficient varied from  $0.025$  ( $L=23H$ ) to  $0.028-0.03$  ( $L=5H$  and  $11H$ ). The free surface profiles calculated from the HEC-RAS and for  $n=0.025$  are plotted in Fig. 9 and the results are compared with experimental data. The HEC-RAS calculation corresponds very well with the measured data.

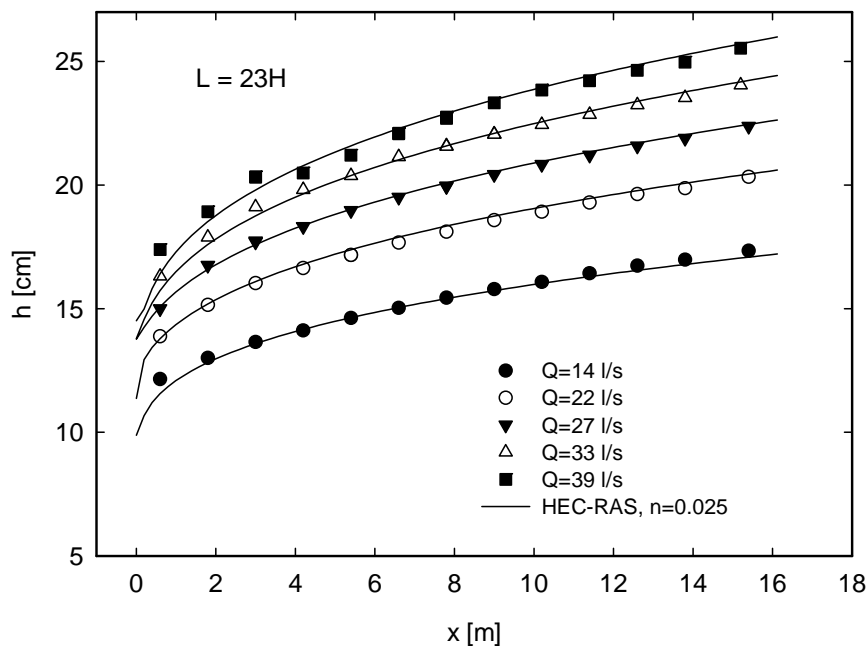


Fig. 9 Free surface profiles – measured and calculated by HEC-RAS

## 5. Conclusion

The influence of surface mounted bars on flow behaviour in the open channel has been evaluated. The bars of the square cross section was placed sequentially on the channel bottom with spacing  $L=5H$ ,  $11H$  and  $23H$ . The profiles of the free surface levels were measured and the numerical simulations were performed. The numerical simulations agree quite well with experimental data for  $L=5H$  and  $11H$ , for the spacing  $L=23H$  the measured data lie slightly above the numerical simulations. From the measured and partially from simulated data the resistance coefficients in the form of drag coefficients and Manning's coefficients were



determined. The drag coefficients are increasing with increasing bar spacing but the total resistance is decreasing with increasing spacing.

## 6. Acknowledgement

The support under the projects No. 103/03/0724 of the Grant Agency of the Czech Republic, and the Institutional Research Plan AV0Z20600510 of ASCR is gratefully acknowledged.

## 7. References

- Morris, H.H. (1959) Design methods for flow in rough conditions. Proc. ASCE, J. Hyd. Div., 85-HY7, pp. 43-62.
- Okamoto, S., Seo, S., Nakaso, K. & Kawai, I. (1993) Turbulent shear flow and heat transfer over the repeated two-dimensional square ribs on ground plane. J. Fluids Eng. 115, pp. 631-637.
- Casarsa, L. & Arts, T. (2002) Aerodynamic performance investigation of a rib roughened cooling channel flow with high blockage ratio. 11th International Symposium – Application of LDA to Fluid Mechanics, July 8-11, Lisbon, Portugal.
- Kameda, T., Mochizuki, S, Osaka, H. (2004) LDA measurement in roughness sub-layer beneath boundary layer developed over two-dimensional square rough surface. 12th International Symposium – Application of LDA to Fluid Mechanics, July 12-15, Lisbon, Portugal.
- Cui, J., Patel, V.C. & Lin, C.-L. (2003) Large Eddy simulations of turbulent flow in a channel with rib roughness. Int. J. Heat Fluid Flow 24, pp. 372-388.
- Leonardi, S., Orlandi, P., Smalley, R.J., Djendi, L. & Antonia, R.A. (2003) Direct numerical simulations of turbulent channel flow with transverse square bars on one wall. J. Fluid Mech. 491, pp. 229-238.